A simple physical model for simulating turbulent imaging

Guy Potvin*, J. Luc Forand, Denis Dion
Defence Research & Development Canada - Valcartier, 2459 Pie-XI Blvd North,
Quebec City, QC, Canada G3J 1X5

ABSTRACT

We show how to simulate realistic turbulent imagery using only two scalar fields, from which we derive a Gaussian and non-isoplanatic Point-Spread Function (PSF). The first field controls mainly scintillation effects, while the second principally controls image displacements. The model is designed for weak turbulence and is based on the first-order Rytov theory for propagation through turbulence. We explain the physical principles behind the model and justify them using empirical evidence.

Keywords: Imaging, turbulence, simulation, propagation

1. INTRODUCTION

We present a method of numerically simulating turbulence effects on a sequence of images using scalar fields defined over the field-of-view (FOV) of the imager, but that are connected to the random optical turbulence between the object and the imaging system. The use of scalar fields is in contrast to methods that use ray-tracing to simulate turbulence effects on imaging[1]. We do this by first assuming a Gaussian form for the PSF, which reduces the complicated turbulent PSF to a set of six parameters (scintillation, horizontal and vertical displacements and three second-order moments) that are modeled as random but correlated fields defined over the image-coordinates and time. The problem of simulating turbulent imaging is then reduced to the modeling of those moments of the PSF over space and time.

Our first study of the space-time correlations of the first and second moments of the PSF was conducted using imaging data of lights seen across Eckernforde bay in northern Germany[2]. This was done as part of the NATO sponsored trial Validation Measurements on Propagation in the Infrared and Radar (VAMPIRA)[3]. We constructed a mathematical theory describing these correlations for weak optical turbulence and an incoherent target, which was expanded to a theory for turbulent imaging under those conditions[4]. This theory had a number of attractive features, including a displacement vector as the gradient of a scalar field, which eliminated the need to simulate the two components individually. However, it was later shown that the spreads of the PSF are describable as higher-order derivatives of an infinite family of scalar fields[5]. This considerably reduces the practical utility of that theory. In this work we show how we modified the original simulator[4] based on empirically observed properties of optical turbulence, to make it considerably simpler. We start by explaining the physical principles behind the PSF and its moments in Section 2. We show how to implement the simulator model numerically in Section 3, we discuss some issues related to validating the model in Section 4 and we conclude in Section 5.

2. THE POINT-SPREAD FUNCTION

In this section we give a brief overview of the physical assumptions of our model. For a more detailed development, the reader should consult Potvin *et al*.[4]

2.1 Physical principles

We construct our physical model for turbulent imaging using a Huygens-Fresnel principle that is generalized to include propagation through a random medium[6] and is illustrated in Figure 1.

*guy.potvin@drdc-rddc.gc.ca; phone 1 418 844-4000 x 4352; fax 1 418 844-4511; www.valcartier.drdc-rddc.gc.ca

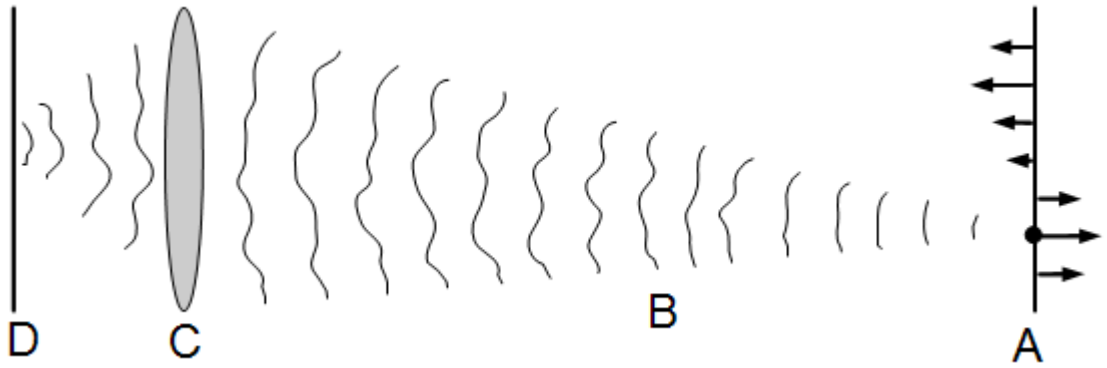

Figure 1. The generalized Huygens-Fresnel principle starts with the electromagnetic field (represented by arrows) at the object plane (A), each point emitting a spherical wave (B) that gets distorted by the atmospheric turbulence. The waves go through a thin lens (C) and are focused on the image plane (D).

We assume that the object plane is a distance L from the lens, which has a diameter D and is a distance f from the image plane. The lens has a focal length f_0 and the image plane is in focus, such that $L^{-1} + f^{-1} = f_0^{-1}$. Without loss of generality, we model the electromagnetic field at the object plane as a scalar field, $E(\vec{\rho}_o)$, where the coordinate vector $\vec{\rho}_o = (x_o, y_o)$ denotes points on the object plane. Each point on the object plane emits a spherical wave that is perturbed by the turbulence on its way to the lens. We use the Rytov approximation for weak turbulence, which is a multiplicative approach, such that

$$E' = E_0 \exp[\psi], \tag{1}$$

where E' represents the perturbed wave, E_0 is the unperturbed incident wave and $\psi = \chi + iS$ is the total perturbation, where χ is the natural logarithm of the multiplicative amplitude perturbation and S is the phase perturbation. After the spherical waves pass through the lens, they are refocused on the image plane. The generalized Huygens-Fresnel approach allows a simple description of the optical system in terms of a transfer function m. The electromagnetic field in the image plane is related to the field in the object plane by a linear integral transformation,

$$E_i(\vec{\alpha}_i) = \int \mathrm{d}^2\alpha_o \, m(\vec{\alpha}_o, \vec{\alpha}_i) E_o(\vec{\alpha}_o), \tag{2}$$

where for convenience we have used a normalized object coordinate, $\vec{\alpha}_o = \vec{\rho}_o / L$, and a normalized image coordinate, $\vec{\alpha}_i = \vec{\rho}_i / f$. Using the small angle approximation, the transfer function is given as,

$$m(\vec{\alpha}_o, \vec{\alpha}_i) = G \exp\left[ik\left(L\alpha_o^2 + f\alpha_i^2\right)/2 \right] \int \mathrm{d}^2\rho_l \, W(\vec{\rho}_l) \exp\left[ik\vec{\rho}_l \cdot (\vec{\alpha}_i - \vec{\alpha}_o) + \psi(\vec{\alpha}_o, \vec{\rho}_l) \right], \tag{3}$$

where G is a normalizing constant, $k = 2\pi/\lambda$ is the radiation wavenumber and $W(\vec{\rho}_l)$ is the characteristic function of the lens such that $W = 1$ when $|\vec{\rho}_l| \le D/2$ and $W = 0$ otherwise. The irradiance received at the image plane is proportional to the squared amplitude of the image electromagnetic field, $I_i \propto E_i E_i^*$. Using Eq (2), we obtain

$$I_i(\vec{\alpha}_i) = \int \mathrm{d}^2\alpha_o \int \mathrm{d}^2\alpha_o' \, m(\vec{\alpha}_o, \vec{\alpha}_i) m^*(\vec{\alpha}_o', \vec{\alpha}_i) \Gamma_o(\vec{\alpha}_o, \vec{\alpha}_o'), \tag{4}$$

where we have defined the Mutual Coherence Function (MCF) which is a function of two object coordinates, $\vec{\alpha}_o$ and $\vec{\alpha}_o'$,

$$\Gamma_o(\vec{\alpha}_o, \vec{\alpha}_o') = \left\langle E_o(\vec{\alpha}_o) E_o^*(\vec{\alpha}_o') \right\rangle_o. \tag{5}$$

The angle brackets represent the average over the ensemble of object electromagnetic fields. The randomness of the object field is distinct and independent from the randomness of the turbulent refractive index field. This is because the object field is taken to be produced by physical processes independent from the turbulence. If the source is self-radiating, such as a Black Body, then the field at the object's surface is random due to thermal fluctuations. If, on the other hand,

the object is lit by a secondary source, then the randomness may be due to the object's surface roughness. We will only consider incoherent objects. This means that the phase of the electromagnetic field at the object's surface is random and is virtually uncorrelated over distances equal or larger than the radiation's wavelength. Since the size of the object is typically much larger than the wavelength, we can approximate the MCF as,

$$\Gamma_o\left(\vec{\alpha}_o,\vec{\alpha}_o'\right)\propto I_o\left(\left(\vec{\alpha}_o+\vec{\alpha}_o'\right)/2\right)\delta\left(\vec{\alpha}_o-\vec{\alpha}_o'\right), \tag{6}$$

in which case Eq (4) becomes,

$$I_i\left(\vec{\alpha}_i\right)=\int \mathrm{d}^2\alpha_o P\left(\vec{\alpha}_o,\vec{\alpha}_i\right) I_o\left(\vec{\alpha}_o\right). \tag{7}$$

The function P is the PSF;

$$P\left(\vec{\alpha}_o,\vec{\alpha}_i\right)=G^2\int \mathrm{d}^2\rho_l\int \mathrm{d}^2\rho_l' W\left(\vec{\rho}_l\right)W\left(\vec{\rho}_l'\right)\exp\left[ik\left(\vec{\rho}_l-\vec{\rho}_l'\right)\cdot\left(\vec{\alpha}_i-\vec{\alpha}_o\right)+\psi\left(\vec{\alpha}_o,\vec{\rho}_l\right)+\psi^*\left(\vec{\alpha}_o,\vec{\rho}_l'\right)\right]. \tag{8}$$

2.2 The zero and first order moments of the PSF

The PSF in Eq (8) depends on the turbulent wave perturbation and so is itself a random function. However, in order to model turbulent effects on an image we do not need the detailed shape of the PSF. Instead, we assume that the PSF has a bi-variant Gaussian form. This means we only need to model the zero, first and second-order moments of the PSF, which are also random functions of time and the object coordinate. We start with the zero-order moment;

$$M_0\left(\vec{\alpha}_o\right)=\int \mathrm{d}^2\alpha_i P\left(\vec{\alpha}_o,\vec{\alpha}_i\right). \tag{9}$$

Since we can define the Dirac delta function as $\delta(x)=(2\pi)^{-1}\int \mathrm{d}k\,\exp[ikx]$, it is clear from Eq (8) that the zero-order moment becomes,

$$M_0\left(\vec{\alpha}_o\right)=\left(\frac{2\pi}{k}\right)^2 G^2\int \mathrm{d}^2\rho_l W\left(\vec{\rho}_l\right)\exp\left[2\chi\left(\vec{\alpha}_o,\vec{\rho}_l\right)\right], \tag{10}$$

where we use the fact that $W^2=W$. From now on, it will be convenient to normalize the moments with respect to the non-turbulent zero-order moment, such that

$$M_0\left(\vec{\alpha}_o\right)=\frac{\int \mathrm{d}^2\rho_l W\left(\vec{\rho}_l\right)\exp\left[2\chi\left(\vec{\alpha}_o,\vec{\rho}_l\right)\right]}{\int \mathrm{d}^2\rho_l W\left(\vec{\rho}_l\right)}=\left\langle\exp\left[2\chi\left(\vec{\alpha}_o,\vec{\rho}_l\right)\right]\right\rangle_l. \tag{11}$$

The angle brackets $\langle\cdots\rangle_l$ denote the average over the aperture surface. In the limit of weak turbulence, we obtain the approximation $M_0\approx 1+2\langle\chi\rangle_l$. We can also model the zero-order moment as $M_0=\exp[h]$, where we call h the scintillation field and we approximate $h\approx 2\langle\chi\rangle_l$. By the same reasoning, we obtain the first-order moment with respect to its non-turbulent value,

$$\vec{M}_1\left(\vec{\alpha}_o\right)=\int \mathrm{d}^2\alpha_i\left(\vec{\alpha}_i-\vec{\alpha}_o\right)P\left(\vec{\alpha}_o,\vec{\alpha}_i\right)=-\frac{1}{k}\left\langle\exp\left[2\chi\left(\vec{\alpha}_o,\vec{\rho}_l\right)\right]\vec{\nabla}_l S\left(\vec{\alpha}_o,\vec{\rho}_l\right)\right\rangle_l, \tag{12}$$

where the operator $\vec{\nabla}_l$ is the gradient with respect to $\vec{\rho}_l$. The center-of-mass of the PSF is defined as,

$$\vec{c}\left(\vec{\alpha}_o\right)=\frac{\vec{M}_1\left(\vec{\alpha}_o\right)}{M_0\left(\vec{\alpha}_o\right)}=-\frac{\left\langle\exp\left[2\chi\left(\vec{\alpha}_o,\vec{\rho}_l\right)\right]\vec{\nabla}_l S\left(\vec{\alpha}_o,\vec{\rho}_l\right)\right\rangle_l}{k\left\langle\exp\left[2\chi\left(\vec{\alpha}_o,\vec{\rho}_l\right)\right]\right\rangle_l}, \tag{13}$$

which, in the limit of weak turbulence, becomes,

$$\vec{c}\left(\vec{\alpha}_o\right) \approx -\frac{1}{k}\left\langle \vec{\nabla}_l S\left(\vec{\alpha}_o, \vec{\rho}_l\right)\right\rangle_l . \tag{14}$$

Equation (14) says that the center of the PSF is displaced by an amount proportional to the gradient of the phase perturbation averaged over the aperture surface. It is this displacement that makes a straight line seem wavy in a turbulent image. We shall call the vector field in Eq (14) the displacement field.

We must relate the scintillation and displacement fields to the turbulent refractive index fluctuation field, $n(\vec{r}, t)$, between the object and the imaging system. Given that $\vec{r} = (x, y, z)$, where the z-axis is the line-of-sight between the object and the imager, the object center is located at $\vec{r} = 0$, and the imager is centered at $\vec{r} = (0,0,L)$, the Fourier transform along the plane perpendicular to the line-of-sight of the refractive index fluctuation is

$$N\left(\vec{K}, z, t\right) = \left(\frac{1}{2\pi}\right)^2 \int \mathrm{d}x \int \mathrm{d}y\, n\left(\vec{r}, t\right) \exp\left[-iK_x x - iK_y y\right], \tag{15}$$

where $\vec{K} = \left(K_x, K_y\right)$ is the wavenumber of the refractive index fluctuation. From this we get the following expressions for the log-amplitude and phase perturbations for weak turbulence where only first-order scattering matters.

$$\chi\left(\vec{\alpha}_o, \vec{\rho}_l, t\right) = kL \int_0^1 \mathrm{d}\eta \int \mathrm{d}^2K\, N\left(\vec{K}, L\eta, t\right) e^{i\vec{K}\cdot\vec{\gamma}} \sin\left[\frac{K^2\mu^2\eta\left(1-\eta\right)}{4\pi}\right] \tag{16}$$

$$S\left(\vec{\alpha}_o, \vec{\rho}_l, t\right) = kL \int_0^1 \mathrm{d}\eta \int \mathrm{d}^2K\, N\left(\vec{K}, L\eta, t\right) e^{i\vec{K}\cdot\vec{\gamma}} \cos\left[\frac{K^2\mu^2\eta\left(1-\eta\right)}{4\pi}\right] \tag{17}$$

In the above expressions, we used a normalized line-of-sight coordinate $\eta = z/L$, the Fresnel zone $\mu = \sqrt{L\lambda}$, and the vector $\vec{\gamma} = \eta\vec{\rho}_l + (1-\eta)L\vec{\alpha}_o$. From these, we get expressions for the scintillation and displacement fields,

$$h\left(\vec{\alpha}_o, t\right) = 2kL \int_0^1 \mathrm{d}\eta \int \mathrm{d}^2K\, N\left(\vec{K}, L\eta, t\right) e^{i\vec{K}\cdot\vec{\alpha}_o L(1-\eta)} \beta_1\left(\frac{K\eta D}{2}\right) \sin\left[\frac{K^2\mu^2\eta\left(1-\eta\right)}{4\pi}\right], \tag{18}$$

$$\vec{c}\left(\vec{\alpha}_o, t\right) = -iL \int_0^1 \mathrm{d}\eta \int \mathrm{d}^2K\, N\left(\vec{K}, L\eta, t\right) \vec{K}\eta e^{i\vec{K}\cdot\vec{\alpha}_o L(1-\eta)} \beta_1\left(\frac{K\eta D}{2}\right) \cos\left[\frac{K^2\mu^2\eta\left(1-\eta\right)}{4\pi}\right], \tag{19}$$

where we define the function $\beta_1(x) = 2J_1(x)/x$, in which $J_1(x)$ is the first-order Bessel function, and it represents the effect of averaging over the aperture. In turns out that Eq (19) can be rewritten as the gradient of a scalar function,

$$\vec{c}\left(\vec{\alpha}_o, t\right) = \vec{\nabla}_o \phi\left(\vec{\alpha}_o, t\right), \tag{20}$$

where the operator $\vec{\nabla}_o$ is the gradient with respect to the normalized object coordinate and the *potential displacement*, ϕ, is defined as,

$$\phi\left(\vec{\alpha}_o, t\right) = -\int_0^1 \mathrm{d}\eta \int \mathrm{d}^2K\, N\left(\vec{K}, L\eta, t\right) \left[\frac{\eta}{1-\eta}\right] e^{i\vec{K}\cdot\vec{\alpha}_o L(1-\eta)} \beta_1\left(\frac{K\eta D}{2}\right) \cos\left[\frac{K^2\mu^2\eta\left(1-\eta\right)}{4\pi}\right]. \tag{21}$$

This result is interesting in two ways. First, from a physical point of view, it shows that for weak turbulence the displacements in a turbulent image have no vorticity. Features in the image may be compressed, expanded, or sheared but not rotated. Second, from a modeling point of view, it means we need only generate the potential displacement field and then find its gradient to obtain the displacement field. We do not need to generate both components of the displacement vector field.

2.3 The spreads of the PSF and the uniformity property

We have found a way to describe the scintillation (Eq (18)) and the center of the PSF (Eqs (20) and (21)). We must now find a description for the spreads, which correspond to the normalized second-order moments of the PSF. From an optical perspective, the 'spread' of the PSF is the blur of the image, which can change from one point to another as the spreads change. In terms of the phase perturbation of the previous subsection, the square of the horizontal spread is

$$s_{xx}\left(\vec{\alpha}_o\right) \approx \left(\frac{\lambda}{D}\right)^2 + \frac{1}{k^2}\left\langle\left(\frac{\partial S}{\partial x_l} - \left\langle\frac{\partial S}{\partial x_l}\right\rangle_l\right)^2\right\rangle_l . \tag{22}$$

Similar expressions hold for the square of the vertical spread s_{yy} and the cross-spread s_{xy}. The first term in Eq (22) represents the blur caused by diffraction, which in our model can be replaced by the blur caused by the optical system. The second term is the variance of the gradient of the phase perturbation over the aperture surface. This term has interesting implications. We can suppose that the turbulence creates a random phase perturbation with a certain correlation length scale, r_S, such that within that scale the phase perturbation has a tilt but is otherwise straight. If an imaging system has an aperture diameter $D \ll r_S$, then the gradient of the phase perturbation will be relatively constant over the aperture, resulting in an image with little blur but significant displacements. On the other hand, if $D \gg r_S$ we would get an image with significant blur but little displacement. In addition, these effects are, on average, complimentary in that the average blur plus the variance of the displacement gives a total blur that is independent of the aperture diameter. Therefore, if we have a long sequence of turbulent images, and we were to find the average image, it would show no displacement but a substantial blur that does not depend on the aperture diameter.

In order to model the turbulent blur, we could decompose the phase perturbation into Zernicke polynomials[5]. The coefficients corresponding to the Zernicke polynomials of the same order can be described as functions of second and higher order derivatives of an infinite family of scalar fields, in a manner similar to the displacement being the gradient of the potential displacement. However, such an attempt would significantly complicate our model. Instead, we exploit what we call the uniformity property of optical turbulence, i.e. uniform regions in the object plane stay uniform in the image plane. An example of this effect is evident in Figure 2, which shows sample visible images from turbulent sequences taken as part of the NATO RTG-40 Active Imager Land Field Trials[7] in November 2005. The upper part of Figure 2 shows a black and white panel at 1 km in weak turbulence conditions, whereas the upper part shows the same panel in strong turbulence. In either case, we see the turbulence effects only along the edges. The white and black regions appear remarkably uniform, an impression that is confirmed when we examine the histograms of these pixels over the entire sequence. Mathematically, this means that the integration of the PSF with respect to the object coordinate is a constant (which we take to be unity) no matter how strong the turbulence between the object and the imager;

$$\int \mathrm{d}^2\alpha_o P\left(\vec{\alpha}_o, \vec{\alpha}_i\right) = 1. \tag{23}$$

A physical explanation for the uniformity property can be had by invoking the reciprocity principle. The object plane in Figure 1 emits radiation (rays) in all direction by virtue of its incoherence. Those rays are then perturbed by the turbulence, pass through the lens and arrive at the image plane which absorbs rays coming from all directions. Since the trajectories of the rays are reversible, we can imagine the inverse or reciprocal situation where the image plane emits rays in all directions, which pass through the lens and the turbulence to arrive at the object plane which absorbs rays coming from all directions. In the reciprocal situation, the number of rays passing through the lens and being absorbed by the object plane is the same, no matter the turbulence intensity. And since the number of rays is taken to be proportional to the total intensity, this gives a physical justification for Eq (23). It should be noted that the uniformity property only applies for incoherent objects. A coherent object would emit rays in a certain preferred direction, which in the reciprocal situation means it can only absorb rays coming from the opposite of that direction. Since the turbulence changes the direction of the rays randomly, it is therefore clear that the number of rays absorbed by the object will also vary randomly. If correct, this analysis will have consequences when trying to model active imaging systems. A reflecting surface illuminated by a coherent laser pulse would certainly produce a coherent reflection. Modeling such a case would require a more complete model than the one presented here.

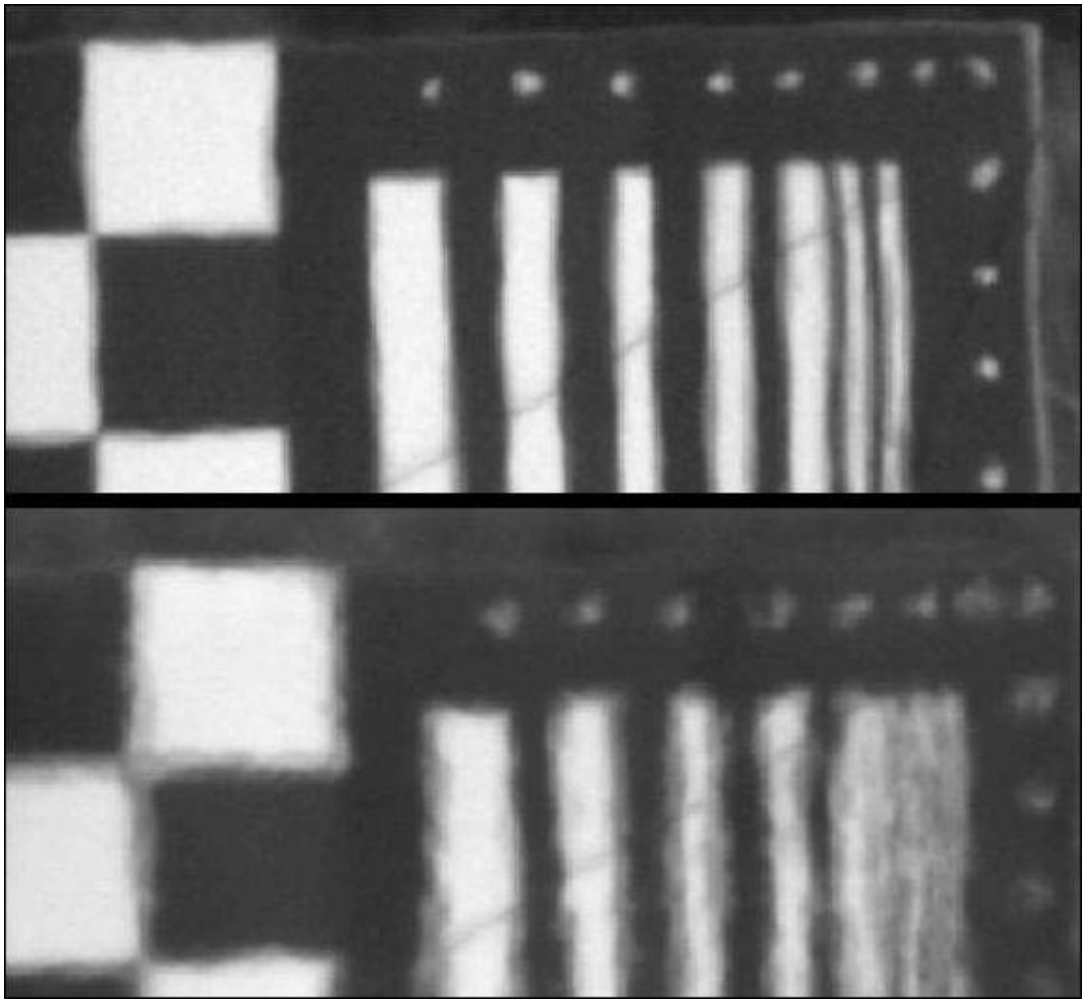

Figure 2. Sample images of a black and white panel at a range of 1 km, recorded with a high-speed digital camera in the visible. The top half shows weak atmospheric turbulence, while the bottom half shows strong turbulence.

The Gaussian bi-variant PSF is represented as,

$$P(\bar{\alpha}_o, \bar{\alpha}_i) = \frac{e^h}{2\pi\sqrt{|\Sigma|}} \exp\left[-\frac{1}{2}\theta_i \Sigma_{ij}^{-1} \theta_j\right], \tag{24}$$

where the Einstein summation convention is used and $\vec{\theta} = (\theta_1, \theta_2) = \vec{\alpha}_i - \vec{\alpha}_o - \vec{c}(\vec{\alpha}_o)$. The spread matrix Σ is

$$\Sigma = \begin{pmatrix} s_{xx} & s_{xy} \\ s_{xy} & s_{yy} \end{pmatrix}, \tag{25}$$

where Σ^{-1} is its inverse, and $|\Sigma|$ the absolute value of its determinant. Now, we make a few simplifications by assuming no scintillation, $h = 0$, and by setting the image coordinate at the origin, $\vec{\alpha}_i = 0$. We further assume that the displacement at the origin is zero, $\vec{c}(0) = 0$, and that about the origin the displacement field is linear;

$$c_i = C_{ij}\alpha_{oj}\,. \tag{26}$$

The matrix *C* is formed from the first-order derivatives of a general displacement field,

$$C=\begin{pmatrix} \dfrac{\partial c_x}{\partial \alpha_{ox}} & \dfrac{\partial c_x}{\partial \alpha_{oy}} \\ \dfrac{\partial c_y}{\partial \alpha_{ox}} & \dfrac{\partial c_y}{\partial \alpha_{oy}} \end{pmatrix}. \tag{27}$$

If the displacement is the gradient of the potential displacement, as in our model, then C is the Hessian of that potential and is symmetric. Given that symmetry, the argument in the exponential of Eq (24) becomes;

$$\theta_i \Sigma_{ij}^{-1} \theta_j = \alpha_{ok} H_{kl} \Sigma_{ij}^{-1} H_{jl} \alpha_{ol}\,, \tag{28}$$

where $H = I + C$ and I is the identity matrix. A natural choice for the spread matrix that compensates for the compression and shear of the displacement field is,

$$\Sigma = \sigma^2 HIH\,, \quad \Sigma_{ij} = \sigma^2 H_{ik}\delta_{kl}H_{lj}\,, \tag{29}$$

where σ^2 is the average blur of the PSF. Then, the individual spreads take the forms,

$$\begin{gathered} s_{xx} = \sigma^2\left[\left(1+\frac{\partial c_x}{\partial \alpha_{ox}}\right)^2 + \frac{\partial c_y}{\partial \alpha_{ox}}\frac{\partial c_x}{\partial \alpha_{oy}}\right], \quad s_{yy} = \sigma^2\left[\left(1+\frac{\partial c_y}{\partial \alpha_{oy}}\right)^2 + \frac{\partial c_y}{\partial \alpha_{ox}}\frac{\partial c_x}{\partial \alpha_{oy}}\right], \\ s_{xy} = \frac{\sigma^2}{2}\left[\left(2+\frac{\partial c_x}{\partial \alpha_{ox}}+\frac{\partial c_y}{\partial \alpha_{oy}}\right)\left(\frac{\partial c_y}{\partial \alpha_{ox}}+\frac{\partial c_x}{\partial \alpha_{oy}}\right)\right]. \end{gathered} \tag{30}$$

It is easy to show that the exponential argument takes on the simple form;

$$\theta_i \Sigma_{ij}^{-1} \theta_j = \alpha_o^2 / \sigma^2\,, \tag{31}$$

such that the PSF is

$$P(\vec{\alpha}_o, \vec{\alpha}_i) = \frac{1}{2\pi\sigma^2}\exp\left[-\frac{1}{2}\theta_i \Sigma_{ij}^{-1}\theta_j\right], \tag{32}$$

and the spreads given in Eq (29) with a linear displacement field will satisfy the uniformity property. However, the PSF in Eq (32) does not give the right scintillation. Integration with respect to the image coordinate gives $\int P \mathrm{d}^2\alpha_i = |H|$ and not e^h as expected. We therefore use the PSF in Eq (24) with the spreads defined in Eq (30). Such a PSF does not satisfy the uniformity property but instead $\int P \mathrm{d}^2\alpha_o = e^h/|H|$. It should be pointed out that $|H| = 1 + \vec{\nabla}_o \cdot \vec{c} + |C|$ and that the divergence of the displacement field is significantly correlated with the scintillation field (evidence of which can be found in Potvin *et al*[2]). This means that the ratio $e^h/|H| \approx 1$ will be close to unity and the uniformity property will be approximately respected. In any case, the uniformity property could only be exact in the case of a linear displacement field, which would never happen. Deviations from uniformity are thus inevitable. In the next section, we will show how to impose the uniformity property on images by a process we call renormalization. What is important is that we used uniformity to obtain expressions (30) for the spreads as functions of the first-order derivatives of the displacement field (which is corroborated by an analysis[8] on the spreads of the turbulent PSF). The expressions (30) dispense with the need for additional scalar fields and considerably simplify the task of modeling.

3. IMPLEMENTING THE MODEL

In this section, we give an overview of the issues concerning the implementation of our model. We will not give detailed instructions on how to produce the turbulence model. Readers interested in greater details should consult Potvin *et al*[4].

3.1 Generating the fields

The position representations of the scintillation (18) and potential displacement (19) fields may be the most natural from a conceptual point of view, but the triple integral they imply is not very practical numerically. Instead we will generate the Fourier representation of these fields. For the scintillation field this turns out to be

$$\mathcal{H}\left(\vec{\kappa}_o,t\right)=\frac{2k}{L}\int_0^1\frac{\mathrm{d}\eta}{\left(1-\eta\right)^2}N\left(\frac{\vec{\kappa}_o}{\left(1-\eta\right)L},L\eta,t\right)\beta_1\left(\frac{\kappa_o\eta D}{2\left(1-\eta\right)L}\right)\sin\left[\frac{\kappa_o^2\mu^2}{4\pi L^2}\frac{\eta}{1-\eta}\right], \tag{33}$$

which has only a single integral. The Fourier representation for the potential displacement is,

$$\mathcal{D}\left(\vec{\kappa}_o,t\right)=-\frac{1}{L^2}\int_0^1\frac{\eta\,\mathrm{d}\eta}{\left(1-\eta\right)^3}N\left(\frac{\vec{\kappa}_o}{\left(1-\eta\right)L},L\eta,t\right)\beta_1\left(\frac{\kappa_o\eta D}{2\left(1-\eta\right)L}\right)\cos\left[\frac{\kappa_o^2\mu^2}{4\pi L^2}\frac{\eta}{1-\eta}\right]. \tag{34}$$

Note that for a given non-zero wavenumber, $\kappa_o>0$, as we go from the object ($\eta=0$) to the imager ($\eta=1$), the fields receive contributions from ever higher turbulent wavenumbers, $K=\kappa_o/(1-\eta)L$. This is due to the fact that the FOV of the imager spreads out like a cone, with its vertex at the imager and its base at the object. Therefore, the fields are sensitive to turbulent eddies that get smaller the closer they are to the imager.

Of course, the images we treat are digital, made up of a discrete array of pixels. If each pixel has an instantaneous field-of-view (IFOV) in radians of φ , then each pixel corresponds to a distance $\varepsilon=L\varphi$ at the object plane. This allows us to define a pixel coordinate $\vec{\alpha}_p=\vec{\alpha}_o(L/\varepsilon)$, with a corresponding pixel wavenumber $\vec{\kappa}_p=\vec{\kappa}_o(\varepsilon/L)$ that leads us to rewrite Eqs (33) and (34) as,

$$\mathcal{H}\left(\vec{\kappa}_p,t\right)=\frac{2kL}{\varepsilon^2}\int_0^1\frac{\mathrm{d}\eta}{\left(1-\eta\right)^2}N\left(\frac{\vec{\kappa}_p}{\left(1-\eta\right)\varepsilon},L\eta,t\right)\beta_1\left(\frac{\kappa_p\eta D}{2\left(1-\eta\right)\varepsilon}\right)\sin\left[\frac{\kappa_p^2\mu^2}{4\pi\varepsilon^2}\frac{\eta}{1-\eta}\right], \tag{35}$$

$$\mathcal{D}\left(\vec{\kappa}_p,t\right)=-\frac{L^2}{\varepsilon^4}\int_0^1\frac{\eta\,\mathrm{d}\eta}{\left(1-\eta\right)^3}N\left(\frac{\vec{\kappa}_p}{\left(1-\eta\right)\varepsilon},L\eta,t\right)\beta_1\left(\frac{\kappa_p\eta D}{2\left(1-\eta\right)\varepsilon}\right)\cos\left[\frac{\kappa_p^2\mu^2}{4\pi\varepsilon^2}\frac{\eta}{1-\eta}\right]. \tag{36}$$

We make simplifications regarding the turbulence by assuming it is a homogeneous, isotropic Gaussian random field that is frozen and advected past the imager by a constant transverse wind $\vec{U}$. This implies that

$$N\left(\vec{K},L\eta,t\right)=N\left(\vec{K},L\eta\right)\exp\left[-i\vec{K}\cdot\vec{U}t\right]. \tag{37}$$

We further assume that the turbulence has an outer scale, L_O, which is roughly its de-correlation length. If $L_O\ll L$, then we can suppose that the turbulence is a succession of roughly $N_s\approx L/L_O$ independent slabs and the refractive index fluctuation can be modeled as having the following correlation function;

$$\overline{N\left(\vec{K},L\eta\right)N^*\left(\vec{K}',L\eta'\right)}\approx\frac{2\pi}{L}\Phi_n\left(\frac{\vec{K}+\vec{K}'}{2},0\right)\delta\left(\vec{K}-\vec{K}'\right)\delta\left(\eta-\eta'\right). \tag{38}$$

The overbar in Eq (38) represents the average over the turbulent fluctuations and Φ_n is the three-dimensional power spectrum of the turbulent refractive index fluctuation,

$$\Phi_n\left(\vec{K}\right)=0.033C_n^2\left(K_O^2+K^2\right)^{-11/6}\Lambda\left(Kl_o\right), \tag{39}$$

where C_n^2 is the refractive index structure parameter, $K_O=2\pi/L_O$ is the wavenumber corresponding to the outer scale, and l_o is the inner scale of the turbulence. The function Λ is the inner scale function that suppresses the power spectrum at scales smaller than the inner scale;

$$\Lambda(x) = \exp\left[-1.28x^2\right] + 1.45\exp\left[-0.97\left(\ln(x) - 0.45\right)^2\right]. \tag{40}$$

Note that the model can accept a refractive index structure parameter $C_n^2(\eta)$, outer scale $L_O(\eta)$ and inner scale $l_o(\eta)$ that are functions of the line-of-sight coordinate.

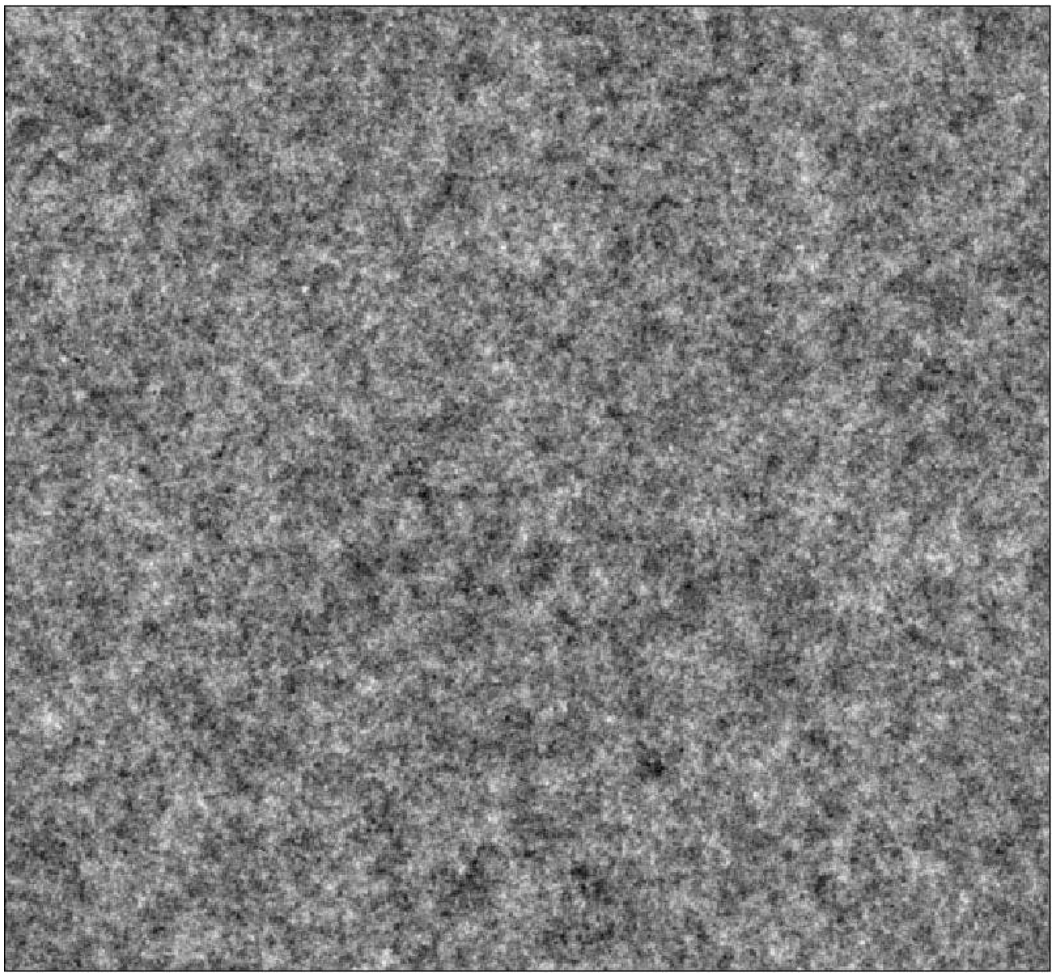

Figure 3. A sample scintillation field created using atmospheric data, corresponding to weak turbulence conditions, taken at the NATO RTG-40 field trial.

The actual numerical generation of the fields is rather elaborate[4]. Suffice to say that we typically want to simulate turbulence on a digital image that is N_i pixels wide and N_j pixels high. Therefore, instead of performing continuous Fourier transforms, we perform Discrete Fourier Transforms (DFT), which give us an $N_i \times N_j$ array of discrete wavenumbers, and instead of the integrals we see in Eqs (35) and (36) we perform a summation over the N_s independent turbulent slabs. For each discrete wavenumber and slab we generate a complex number representing the complex amplitude of the partial Fourier transform of the refractive index fluctuation. This number has a mean of zero, the real and imaginary parts are independent, and both are normally distributed with the same variance. The variance is proportional to the refractive index power spectrum for that specific wavenumber and slab position. However, this method generates fields that are continuous at opposite ends of the image. In other words, the values at one edge of the field are identical to those at the opposite edge. We compensate for this by generating fields that are twice the size of the image, then cropping the fields by half so that they have the same size as the image. Figures 3 and 4 show sample

scintillation and potential displacement fields, respectively, for atmospheric conditions consistent with those of the weak turbulence case shown in the upper half of Figure 2.

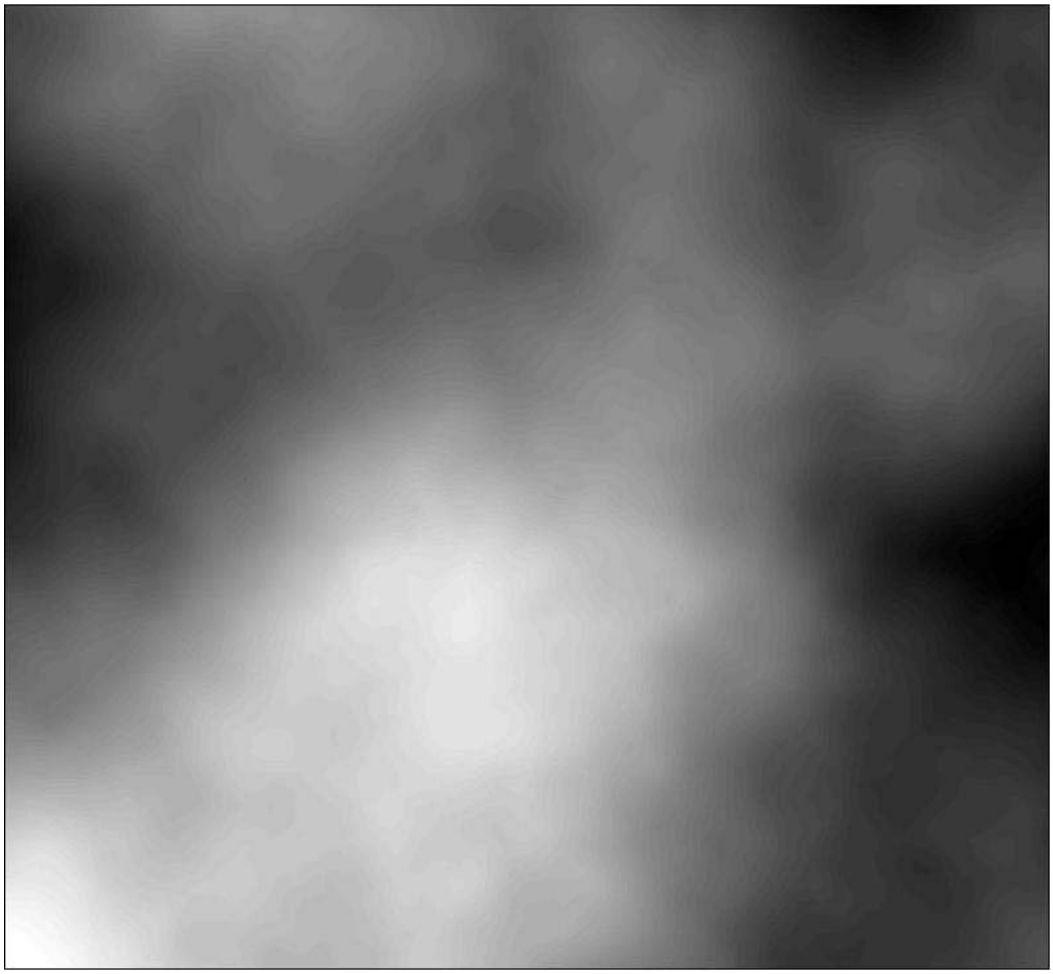

Figure 4. A sample potential displacement field created using the same atmospheric data as in Figure 3.

3.2 Generating the image

We are now ready to generate an image. The potential displacement field in Figure 4 generates the displacement field and the spreads according to Eq (30) and forms the morphology of the PSF, shown in Figure 5. There, we see an array of ellipses with small crosses inside. The ellipses represent the way the PSF redistributes the intensity coming from a point in the object plane, itself represented by the cross. The shapes of the ellipses are determined by the spreads in Eq (30), using the derivatives of the displacement field evaluated at the crosses. The fact that the ellipses are not centered about their crosses illustrates the effect of the displacement. Both the displacements and the variable spreading have been magnified for the sake of the illustration.

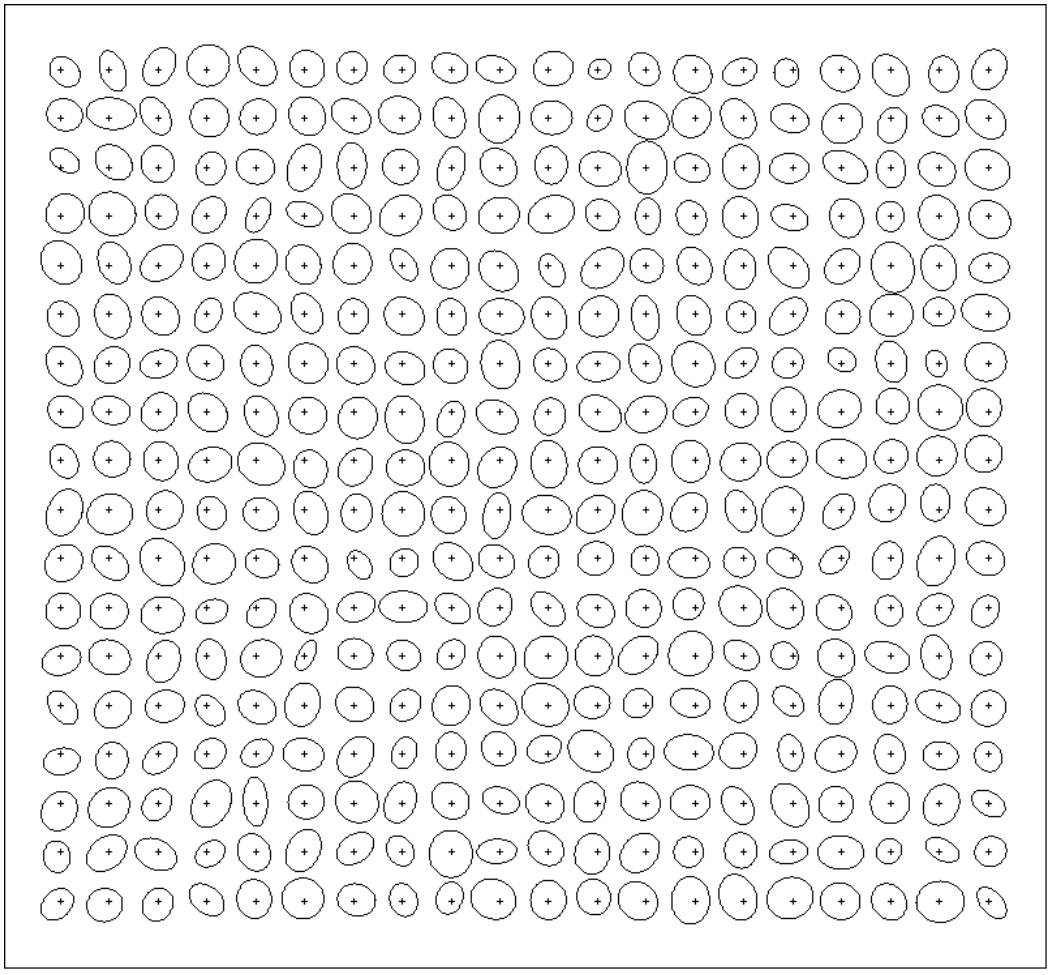

Figure 5. An illustration of the morphology of the PSF derived from the potential displacement field shown in Figure 4.

We find it more convenient to produce the Fourier transform of the image rather than the image itself. Once we have the Fourier transform of the turbulent image, we perform an inverse transform to obtain the actual turbulent image. As the Fourier transform of the image is given by

$$F_i\left(\vec{\kappa}_i\right)=\left(\frac{1}{2\pi}\right)^2\int \mathrm{d}^2\alpha_i\, I_i\left(\vec{\alpha}_i\right)\exp\left[-i\vec{\kappa}_i\cdot\vec{\alpha}_i\right], \tag{41}$$

then Eq (7) becomes,

$$F_i\left(\vec{\kappa}_i\right)=\left(\frac{1}{2\pi}\right)^2\int \mathrm{d}^2\alpha_o P\left(\vec{\alpha}_o,\vec{\kappa}_i\right) I_o\left(\vec{\alpha}_o\right), \tag{42}$$

where

$$P\left(\vec{\alpha}_o,\vec{\kappa}_i\right)=\exp\left[h\left(\vec{\alpha}_o\right)-\frac{1}{2}\kappa_{in}\Sigma_{nm}\left(\vec{\alpha}_o\right)\kappa_{im}-i\vec{\kappa}_i\cdot\left(\vec{\alpha}_o+\vec{c}\left(\vec{\alpha}_o\right)\right)\right]. \tag{43}$$

However, as we explained earlier, the image obtained from Eqs (41) to (43) does not respect the uniformity property. We therefore enforce this property by creating a reference image, $I_R(\vec{\alpha}_i)$, that is a perfectly flat image of intensity unity and is put through the same treatment as the object. The Fourier transform of the reference image is

$$F_R\left(\vec{\kappa}_i\right)=\left(\frac{1}{2\pi}\right)^2\int \mathrm{d}^2\alpha_o P\left(\vec{\alpha}_o,\vec{\kappa}_i\right). \tag{44}$$

We obtain the final image by taking the ratio of the image to the reference image;

$$I_F\left(\vec{\alpha}_i\right)=\frac{I_i\left(\vec{\alpha}_i\right)}{I_R\left(\vec{\alpha}_i\right)}=\frac{\int \mathrm{d}^2\alpha_o P\left(\vec{\alpha}_o,\vec{\alpha}_i\right) I_o\left(\vec{\alpha}_o\right)}{\int \mathrm{d}^2\alpha_o P\left(\vec{\alpha}_o,\vec{\alpha}_i\right)}, \tag{45}$$

where it is easy to see that in regions where the object is constant, $I_o = \text{const}$, the final image equals the same value, $I_F = \text{const}$.

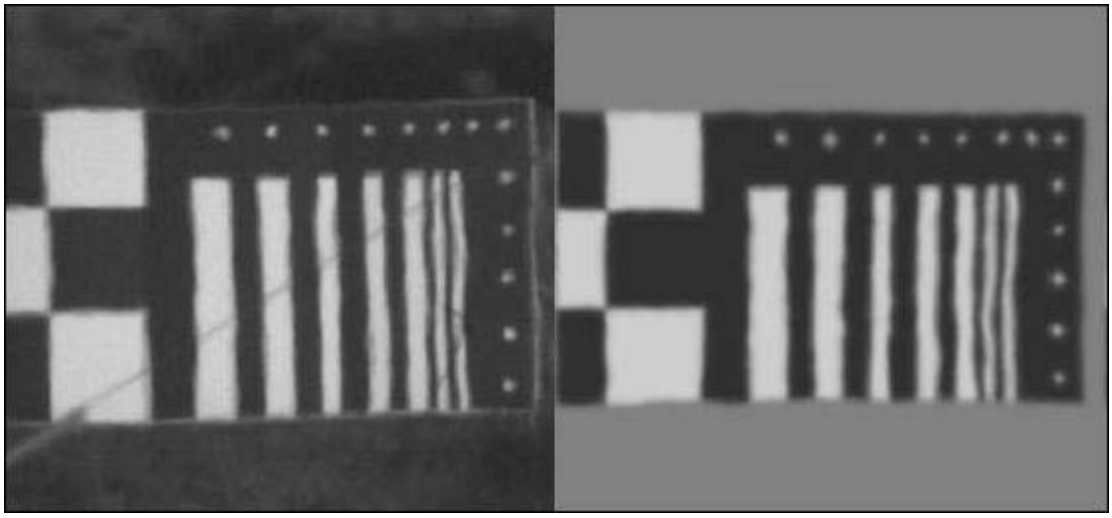

Figure 6. A comparison between a sample image from the weak turbulence case seen in Figure 2 (left) and an output image produced by our model using comparable atmospheric conditions (right).

Although Eq (45) is valid mathematically, it is not suitable numerically. It turns out the cancellation in a flat region is not perfect. We correct for this by dividing the object into its mean value and the deviation from that mean: $I_o(\vec{\alpha}_o) = M + \Delta I_o(\vec{\alpha}_o)$. We then apply Eq (42) to the deviation,

$$\Delta F_i\left(\vec{\kappa}_i\right)=\left(\frac{1}{2\pi}\right)^2\int \mathrm{d}^2\alpha_o P\left(\vec{\alpha}_o,\vec{\kappa}_i\right)\Delta I_o\left(\vec{\alpha}_o\right), \tag{46}$$

from which we obtain a deviatory turbulent image, $\Delta I_i(\vec{\alpha}_i)$. The final image then becomes

$$I_F\left(\vec{\alpha}_i\right)=M+\frac{\Delta I_i\left(\vec{\alpha}_i\right)}{I_R\left(\vec{\alpha}_i\right)}=M+\frac{\int \mathrm{d}^2\alpha_o P\left(\vec{\alpha}_o,\vec{\alpha}_i\right)\Delta I_o\left(\vec{\alpha}_o\right)}{\int \mathrm{d}^2\alpha_o P\left(\vec{\alpha}_o,\vec{\alpha}_i\right)}, \tag{47}$$

which is displayed on the right side of Figure 6.

4. DISCUSSION ON MODEL VALIDITY

While the simulated image in Figure 6 may look convincing, there remains the question of validating the model. This is problematic since, even on the simplified terms of the model, the process of producing a perturbed image is complex. A turbulent image depends on the entire profile of outer scale, inner scale, and C_n^2 from the object to the sensor. Therefore, even if there is a slight disagreement between real data and the simulator output, it would be possible to alter the profiles in such a way as to obtain agreement. This is particularly true in a measurement trial, since measures of turbulence and atmospheric conditions are typically taken at one location. Thus one can always plausibly adjust the profiles to obtain a better agreement with imaging data and still be consistent with the atmospheric data. A proper validation would therefore need turbulent imaging data taken in controlled indoor conditions. The optical turbulence would be artificially generated and adequately measured. With such a set-up one could also obtain a pristine image of the target without turbulence that can be altered with the simulator and compared with the experimental image.

5. CONCLUSIONS AND FUTURE WORK

We have shown how to simulate the effects of weak optical turbulence on an imaging system looking at an incoherent target. The model first generates a turbulent field of index of refraction fluctuations. From this, it derives two scalar fields defined over the FOV of the imager, the scintillation and the potential displacement fields, which are then used to derive all six moments of a bi-variant Gaussian PSF. After applying this PSF to the unperturbed image in the correct way (removal of the mean and renormalization), we obtain a turbulent image that compares well to imaging data (Figure 6).

In addition to validating the model, we must also find ways to extend it to simulate coherent targets and strong turbulence conditions. As mentioned previously, a coherent target would invalidate the uniformity property, but is necessary in order to model reflective surfaces on a target and/or active imaging systems. Extending the model to strong optical turbulence is necessary to be able to simulate any and all atmospheric conditions, but will likely be difficult since the first-order Rytov theory would no longer be applicable.

REFERENCES

[1] Tofsted, D. H., “Turbulence modeling: On phase and deflector screen generation,” U.S. Army Research Laboratory Technical Report, ARL-TR-1886 (2001).

[2] Potvin, G., Forand, J. L., Dion, D., “Some space-time statistics of the turbulent point-spread function,” J. Opt. Soc. Am. A, Vol. 24, 753-763 (2007a).

[3] Final Report of Task Group SET-056, "Integration of radar and infrared," NATO Research and Technology Organization Technical Report, TR-SET-056 (2009).

[4] Potvin, G., Forand, J. L., Dion, D., "A parametric model for simulating turbulence effects on imaging systems," Defence Research & Development Canada – Valcartier Technical Report, TR 2006-787 (2007b).

[5] Potvin, G., Forand, J. L., Dion, D., “Some theoretical aspects of the turbulent point-spread function,” J. Opt. Soc. Am. A, Vol. 24, 2932-2942 (2007c).

[6] Fante, R. L., “Wave propagation in random media: A systems approach,” In Wolf, E., (Ed.), Progress in Optics, Vol. XXII, Elsevier Science Publishers, Amsterdam, North-Holland, 341-398 (1985).

[7] Tofsted, D. H., Quintis, D., O’Brien, S., Yarbrough, J., Bustillos, M., Tirrell Vaucher, G., “Test report of the November 2005 NATO RTG-40 Active Imager Land Field Trials,” U.S. Army Research Laboratory Technical Report, ARL-TR-4010 (2006).

[8] Brosset Heckel, D., “Analyse des effets de l’étalement turbulent sur l’imagerie,” Internship report, Écoles de Saint-Cyr, Coëtquidan, France (2008).